EFFECT OF MATERIALS HETEROGENEITIES ON MICROSTRUCTURE AND MECHANICAL PROPERTIES AT IRRADIATED STATE

Authors

Frank Bergner, Hans-Werner Viehrig (HZDR)

Contributors of Task 3.3 (CIEMAT, CNRS, Framatome, NRI, VTT)

This project received funding under the Euratom research and training programme 2014-2018 under grant agreement Nº 661913

Content

- Material FZD-4 (HZDR + CIEMAT)
  - basic information, initial microstructure and properties
  - irradiation-induced microstructure and property changes
- Material EDF-4 (CNRS)
  - basic information, initial microstructure and properties
  - irradiation-induced microstructure
- Materials NRI-1/2 (NRI)
  - basic information, initial microstructure and properties
  - irradiation hardening
- Materials ANP-3/4 + VTT-1/WM1 (VTT + Framatome)
  - basic information
  - MC and cleavage initiation sites for irradiated condition

FZD-4: basic information (1)

- NPP Greifswald, RPV of Unit 8, VVER440-type base metal 15Kh2MFAA
- RPV of Unit 8 completed in 1989 (Škoda production), non-commissioned
- Identical in construction with operating NPPs at Dukovany, Bohunice, Mochovce, Paks

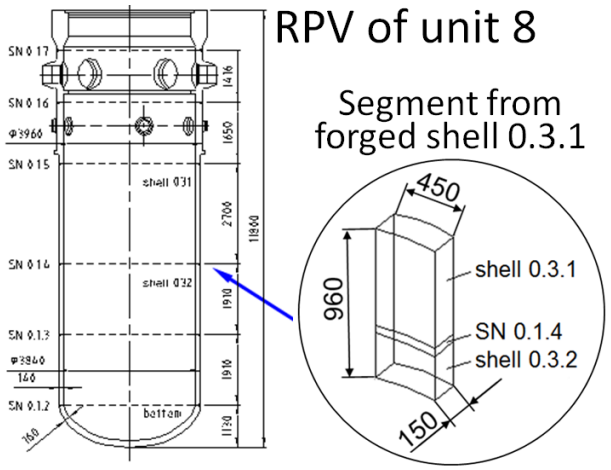

Composition of 15Kh2MFAA forged ring 0.3.1 (wt. %)

	C	Si	Mn	Cr	Ni	Mo	Cu	P	V
HZDR analysis	0.15	0.30	0.45	2.86	0.10	0.79	0.05	0.008	0.31
Documentation	0.16	0.25	0.49	2.82	0.09	0.72	0.05	0.01	0.29

FZD-4: basic information (2)

- Irradiated at HFR Petten (LYRA 9) and KFKI Budapest (BAGIRA - Budapest Advanced Gas-cooled Irradiation Rig with Aluminium structure)
- Reported irradiation conditions:

Irradiation experiment	Neutron fluence (10^{19} cm^{-2}) (E > 1 MeV)	Neutron flux (10^{12} $cm^{-2}s^{-1}$) (E > 1 MeV)	Irradiation temperature (°C)	Irradiation time (full power days)
Lyra 9	2.6	1.1	270	272
Bagira C	11.7	34.8	290	49
Bagira A	18.2	54.1	290	49
Bagira B	20.8	61.9	290	49

FZD-4: initial microstructure (1)

- EBSD reveals a bainitic microstructure with former austenite grains (~110 µm), packets (~30 µm) and blocks (9 µm)
- EBSD provides details about the variant selection during the bainitic transformation

Austenite grain boundaries and **block**/**packet** boundaries:

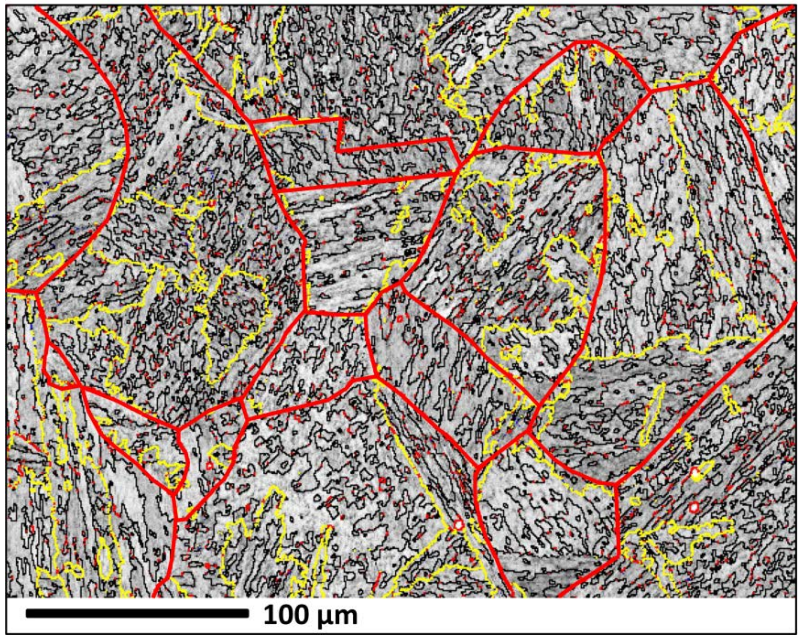

IPF-X plot:

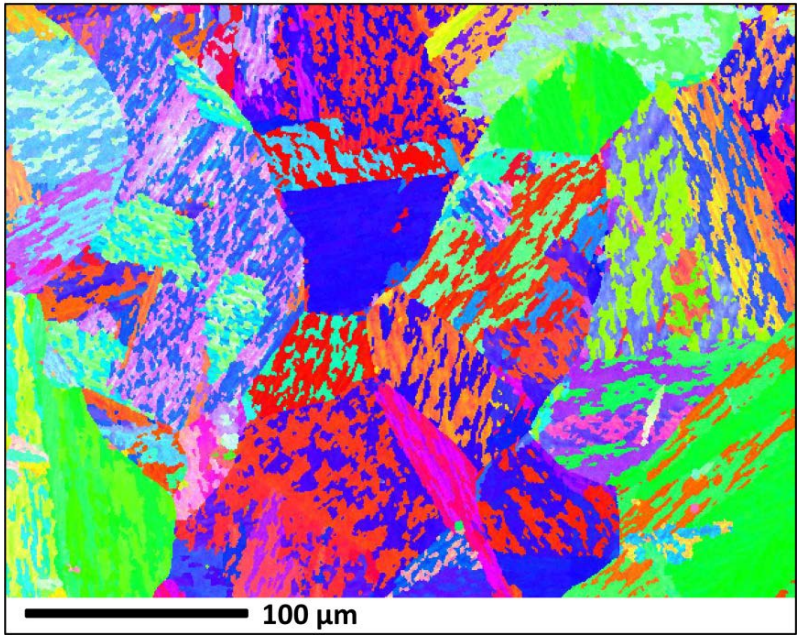

FZD-4: initial microstructure (2)

- Hierarchically organized precipitates and inclusions that differ in their size and density over several orders of magnitude
- Location is related to bainitic grain structure

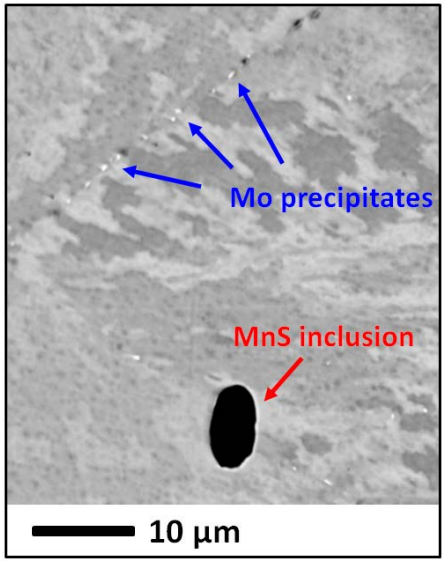

Type	Mean size (µm)	Number density (cm^{-3})	Preferred location
Very small V-rich (TEM)	0.02	2.7E+14	Matrix
V-rich (TEM)	0.14	3.8E+13	Packet/block boundaries
Cr-rich (TEM)	0.2	1.0E+13	Packet/block boundaries
Mo-rich (SEM)	0.4	1E+10	γ-grain boundaries
Coarse MnS (SEM)	8	3E+06	-

- CIEMAT: Spatial variations of dislocation density, mean value ρ = 2.6E+14 m^{-2}

FZD-4: initial properties (1)

- Through-thickness distribution of hardness

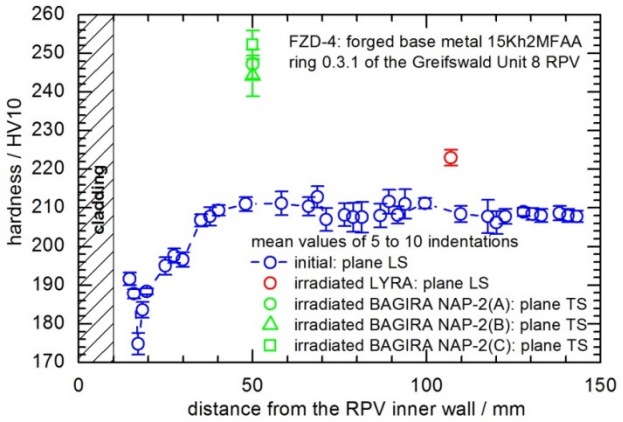

- Through-thickness distribution of MC-T_0 (left) and temperature-adjusted MC for all data (right)

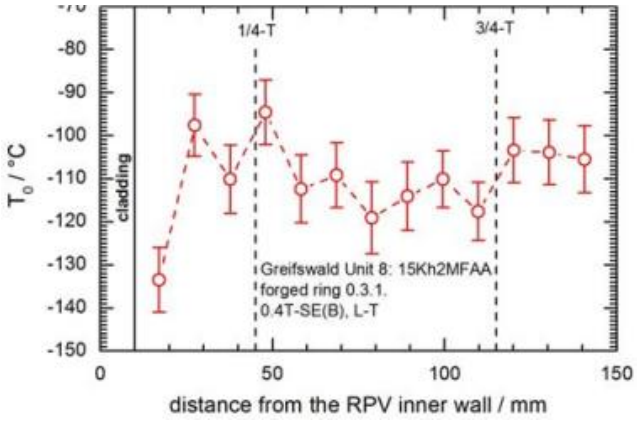

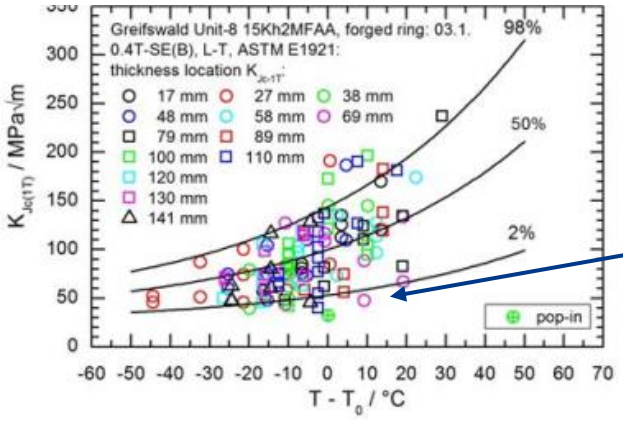

9 out of 98 data points are below the 2% tolerance bound!

FZD-4: initial properties (2)

- Possible reason for large scatter: Local appearance of inter-granular fracture (23% fatigue crack, 11% cleavage crack)

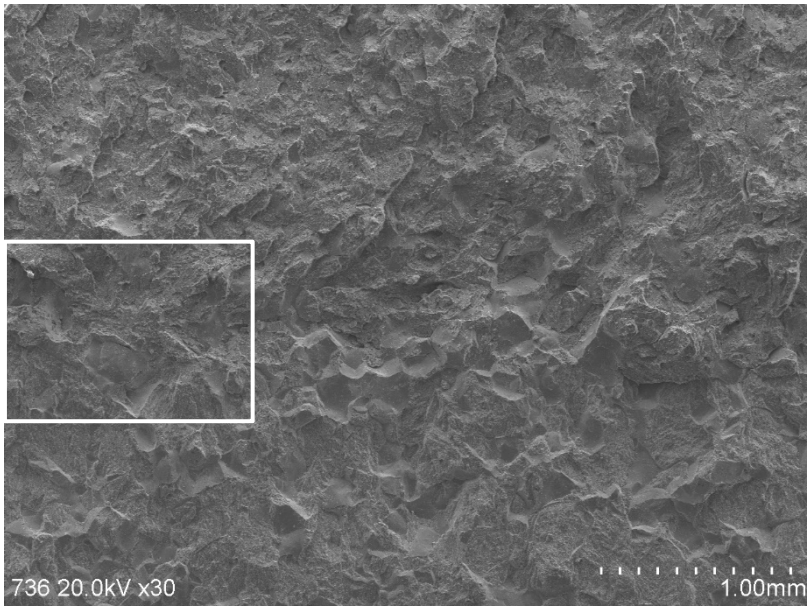

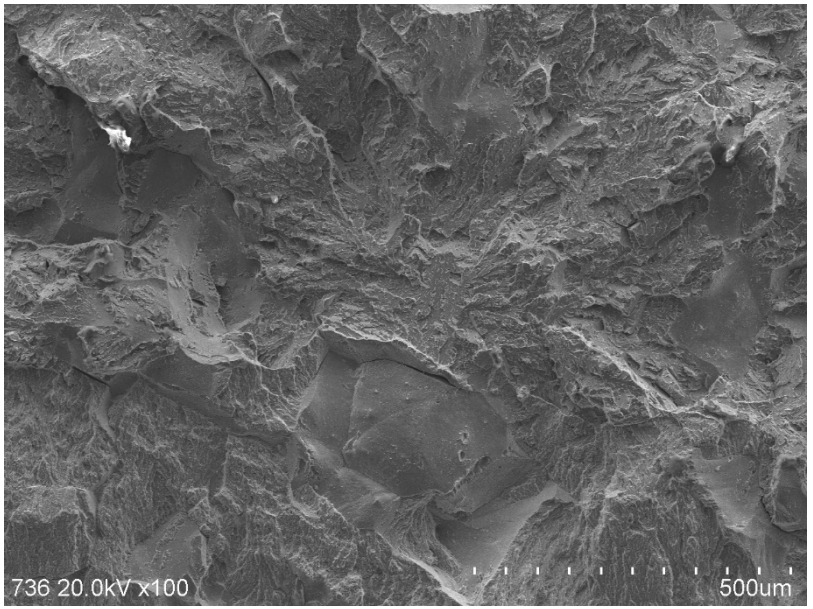

- Consistent with AES evidence (CIEMAT): P enrichment at GBs found at intergranular fracture planes
- Consequence: MC approach not applicable → multimodal MC

FZD-4: irradiated microstructure (1)

- TEM (CIEMAT)
  - BAGIRA (B) irradiation: 20.8E+19 cm^{-2} (E > 1 MeV), 290°C
  - Dislocation loops observed, mostly closely to line dislocations
  - Mean size 1.9 nm, Number density 2E+15 cm^{-3} (g=110)
  - No/very few defects detectable for RPV steels at lower fluences

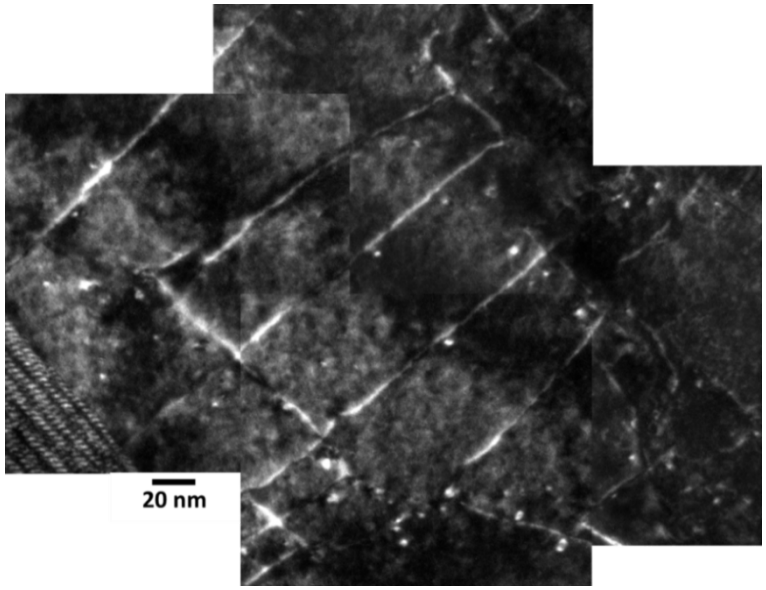

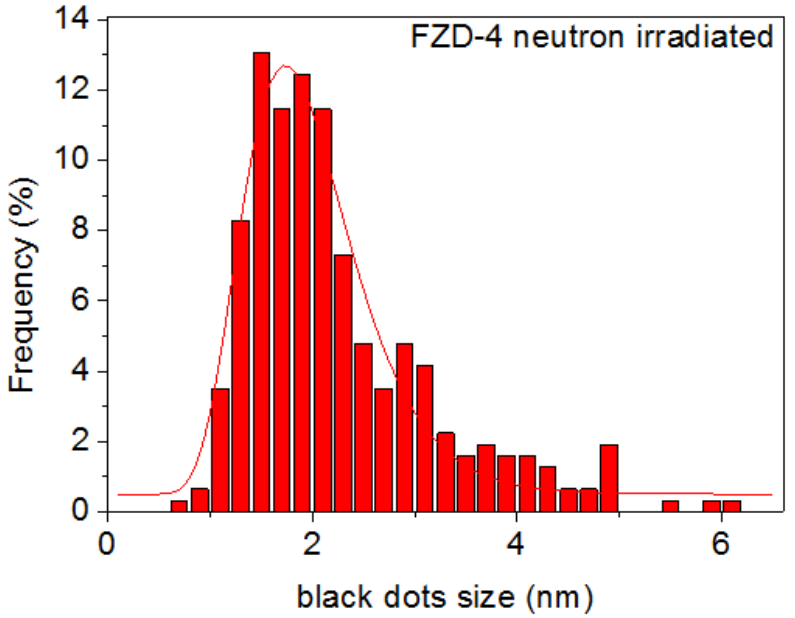

FZD-4: irradiated microstructure (2)

- SANS (HZDR, beamline V4 at HZB Berlin)

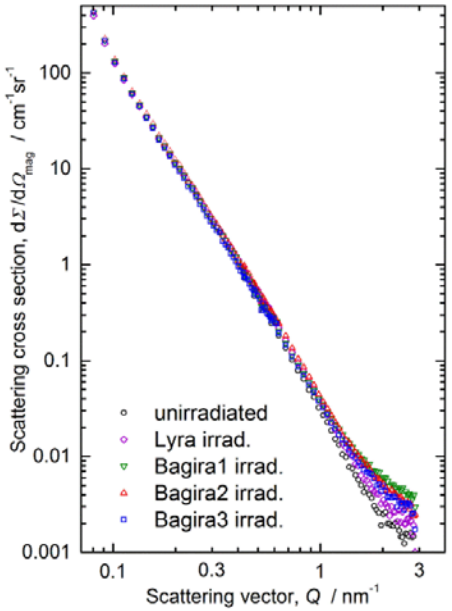

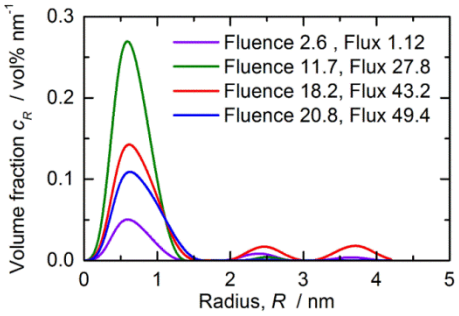

Irradiation experiment	Neutron fluence (10^{19} cm^{-2})	Volume fraction (vol%)	Mean radius (nm)	A-ratio (-)	Vickers hardness, HV10 (-)	ΔHV10 (-)
unirradiated	0	0	-	-	218.5 ± 1.9	0
Lyra	2.6	0.037 ± 0.003	0.83 ± 0.06	1.5 ± 0.2	229.5 ± 3.9	11 ± 5
Bagira (C)	11.7	0.162 ± 0.005	0.76 ± 0.07	2.0 ± 0.2	252.2 ± 3.7	34 ± 5
Bagira (A)	18.2	0.116 ± 0.005	0.78 ± 0.05	3.0 ± 0.5	247.2 ± 3.8	29 ± 5
Bagira (B)	20.8	0.081 ± 0.004	0.78 ± 0.04	2.0 ± 0.2	244.2 ± 5.3	26 ± 6

- BAGIRA irradiations: Decreasing volume fraction at increasing fluence → Contradiction
- Reason: Exp. error? No! // Mix-up of samples? No!

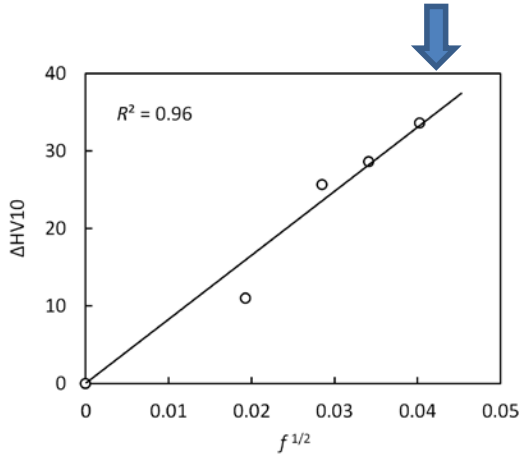

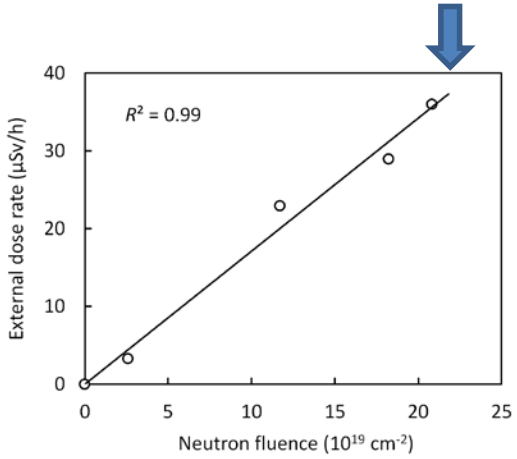

FZD-4: irradiated properties

- MC for LYRA (left) and BAGIRA (right) irradiations

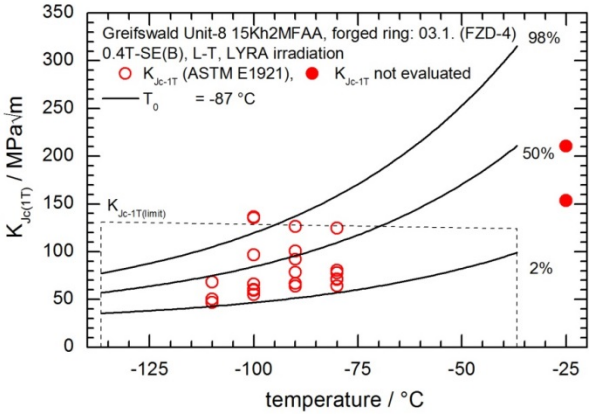

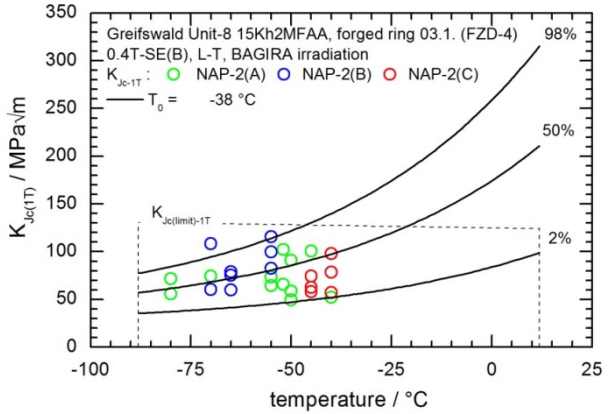

Irradiation experiment	Neutron fluence (10^{19} cm^{-2}) (E > 1 MeV)	Volume fraction (vol%)	ΔHV10 (-)	ΔT_0 (K)
Lyra 9	2.6	0.037	11	24
Bagira C	11.7	0.162	34	97
Bagira A	18.2	0.116	29	80
Bagira B	20.8	0.081	26	61

Data scatter for irr. conditions are smaller than for the initial condition

MC T_0 shift also decreases with increasing fluence

→ any material inhomogeneity can be excluded as reason, because samples were taken from random positions

FZD-4: conclusions

- In the initial condition, large scatter of fracture toughness (MC not applicable) and spatial variations of the fracture mode (inter- or trans-granular) were observed.
- In the as-irradiated condition, the scatter is reduced, intergranular fracture occurs as well.
- The reduction of scatter can be rationalized by the fact that smaller precipitates (available at higher number) may trigger crack initiation for the irradiated condition.
- Reductions of volume fraction, ΔHV10 and ΔT_0 at increasing fluence were observed for BAGIRA. A number of potential reasons have been excluded.

EDF-4: basic information (1)

- EDF-4 is a 16MND5-type RPV steel taken from a shell ring of an RPV manufactured by Creusot-Loire
- Half-Charpy specimen of this material was provided by EDF
- CNRS contribution: comparison between chemical heterogeneities (microsegregations resulting from the solidification versus non-segregated areas)
- Methods: APT and TEM on samples in as-received and ion-irradiated conditions
- Composition:

Material	Range	C	S	P	Si	Mn	Ni	Cr	Mo	V	Cu	Co	Al
EDF4	min	0.69	0.01	0.019	0.42	1.27	0.65	0.20	0.29	0.0087	0.61	0.019	0.045
	max			0.023	0.45	1.34	0.66		0.30	0.010			

EDF-4: basic information (2)

- Ion irradiation at Jannus

Nb.	Sample	Ion	Energy (MeV)	Fluence (10^{14} cm^{-2})	Flux (10^{10} cm^{-2}s^{-1})	Time (min)	Dose at APT analyses depth (dpa)	Dose rate (10^{5} dpa.s^{-1})	T (°C)
1	A239	Fe^{3+}	5	2.85	1.6 ± 0.4	130	~0.1	1.3	400
2 *	4H3.3			8.55	5	296	0.26-0.34	1.7	
2 **							0.78-0.85	4.5	
3	4H3.3			9.5	4.4	360	0.28-0.36	1.4	350

- SRIM calculations of the depth profiles of dpa and injected interstitials

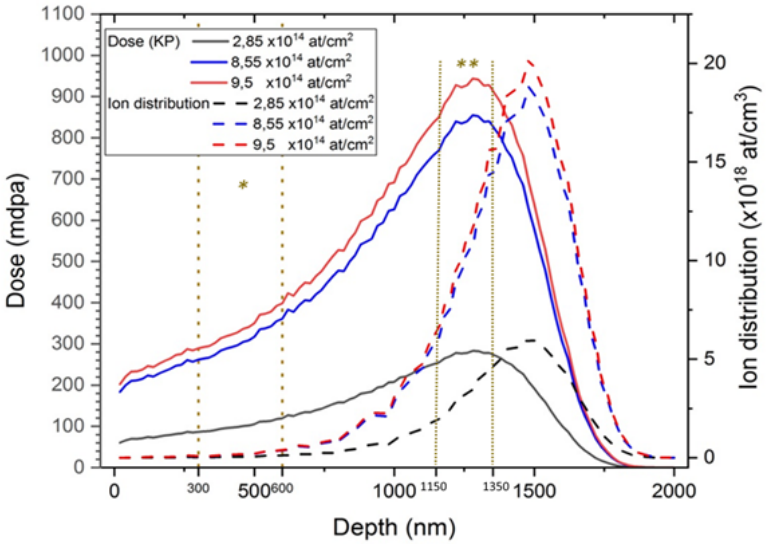

EDF-4: initial microstructure

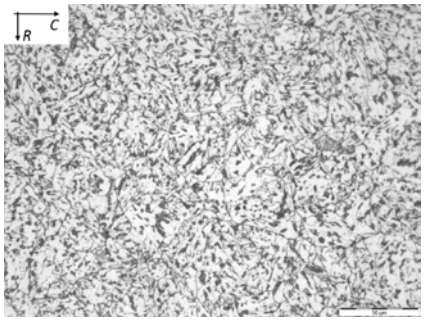

Segregation-free area

Tempered upper bainite

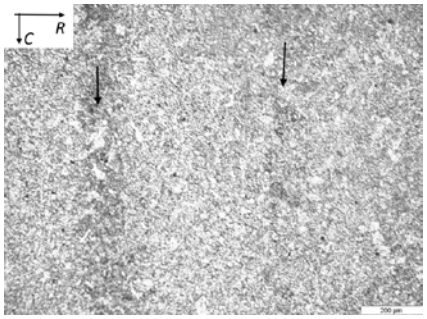

Microsegregations

Tempered lower bainite

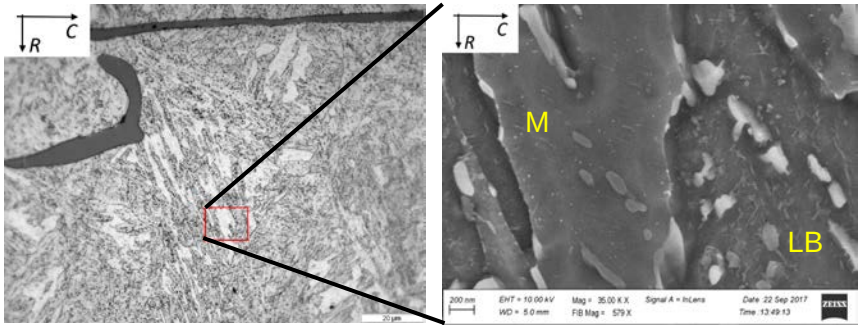

Macrosegregations (ghost lines)

Tempered lower bainite (LB) and tempered martensite (M)

Nano-hardness

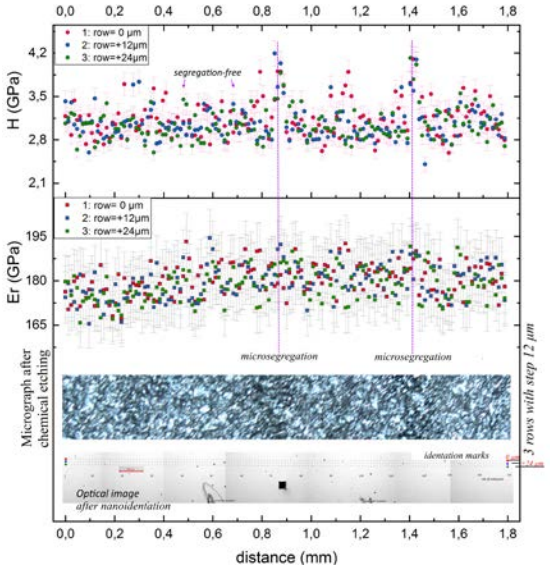

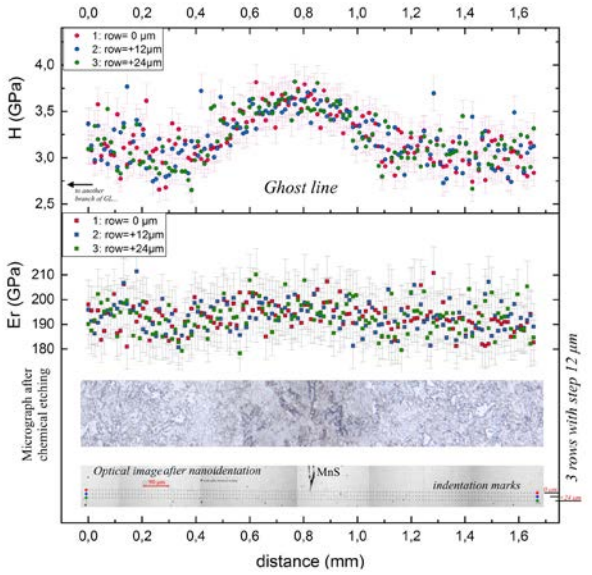

→ FIB lift-out of samples for APT and (S)TEM

EDF-4: irradiated microstructure

- Occasional appearance of
  - NiSiMnP-enriched cluster in ion-irradiated sample from segregation-free area
  - MnNiSiMoCuP-enriched cluster in ion-irradiated sample from microsegregation area
- All ion-irradiated samples
  - P segregation to dislocations and GBs
  - Enrichment of dislocations with Mn, Ni and Si.
- No clear differences in the irradiation response between segregated and segregation-free areas were found.

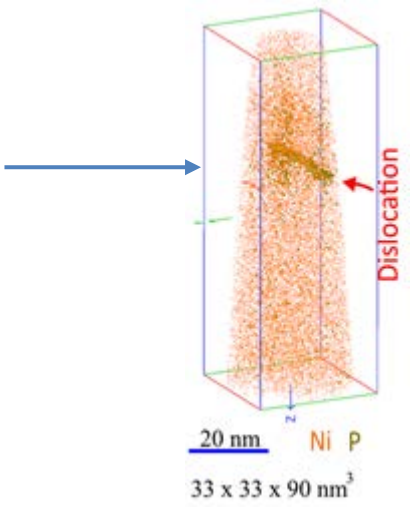

NRI-1 and -2: basic information

NRI-1

- ASTM A 533B type IAEA reference steel known as JRQ,
- 160 t Ingot rolled into plates 225 x 2,500 x 3,000 mm,
- Final heat treatment: normalized at 900 °C, quenched from 880 °C, tempered at 665 °C for 12 hours.

	C	Mn	P	S	Si	Ni	Cr	Mo	Cu	V	Al
5JRQ	0.18	I.47	0.019	0.004	0.24	0.66	0.12	0.5	0.15	0.007	0.014

NRI-2

- 15Kh2NMFAA type RPV steel for the beltline region of WWER-1000,
- Cylindrical ring, thickness 190 mm,
- Final heat treatment: normalized at 950-970 °C, quenched from 910-930 °C, tempered at 660-680 °C, annealed 640 °C.

	C	Mc	Si	S	P	Cr	Ni	Mo	V
15Kh2NMFAA	0.15	0.46	0.22	0.012	0.008	1.54	1.34	0.53	0.12

NRI-1 and -2: initial microstructure

- NRI-1 (JRQ)

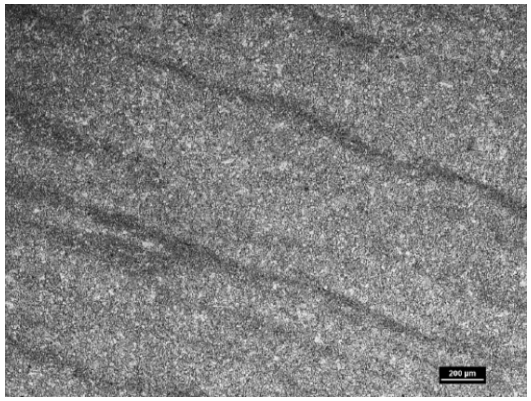
Layer 1 (5 mm depth)

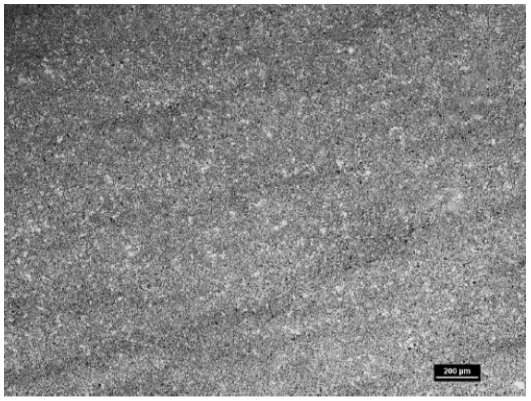
Layer 7 (113 mm depth)

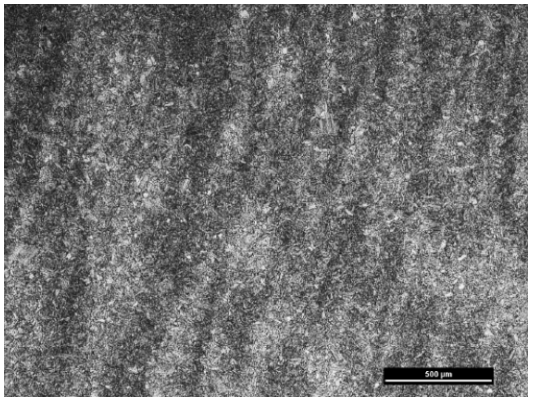
Layer 13 (220 mm depth)

- NRI-2 (15Kh2NMFAA)

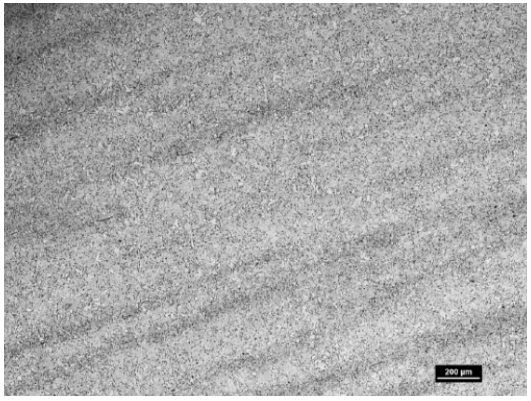
Layer 1 (5 mm depth)

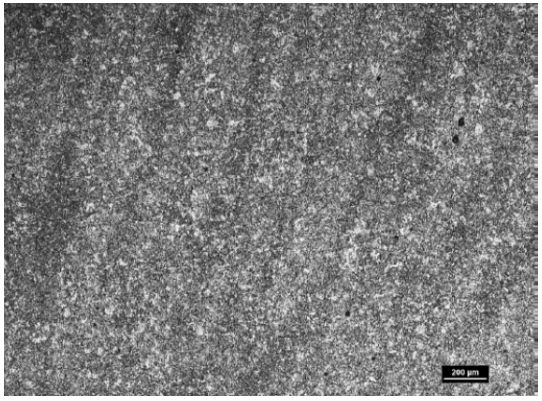
Layer 6 (95 mm depth)

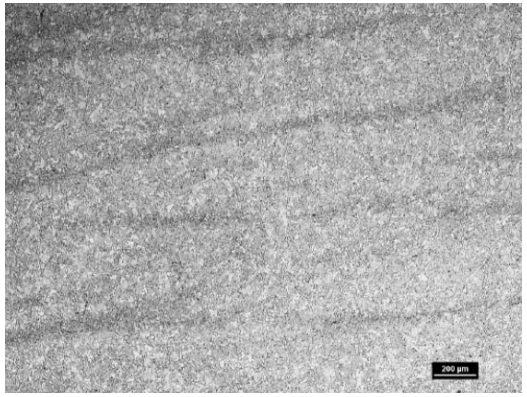
Layer 11 (185 mm depth)

NRI-1 and -2: initial properties

- JRQ
  - characteristic through-thickness profile of HV0.1
  - Segregation bands (270 HV0.1) harder than base (210 HV0.1)

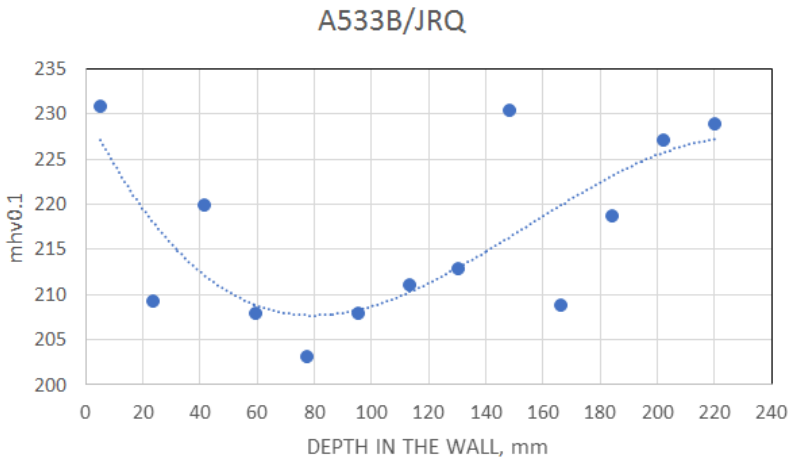

- 15Kh2NMFAA
  - HV0.1 approximately const.

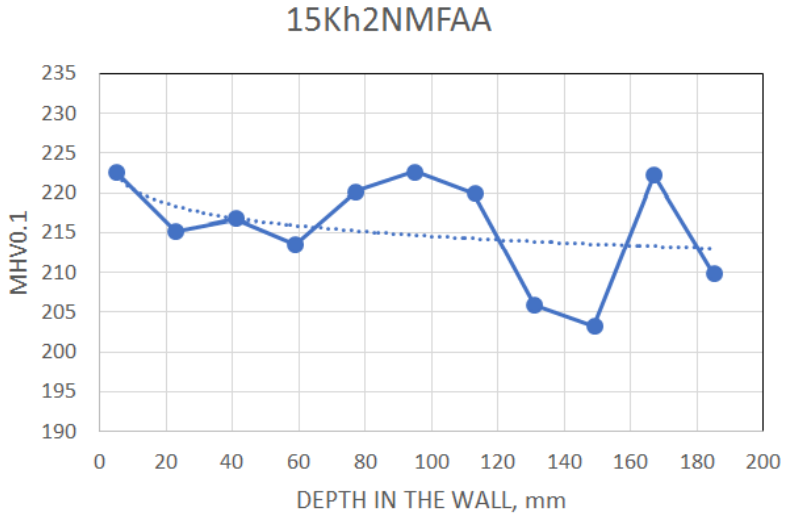

NRI-1 and -2: irradiation hardening

- JRQ
  - Irradiation-induced increase of HV0.1
  - ΔHV0.1 almost equal for segregation bands and segregation-free area

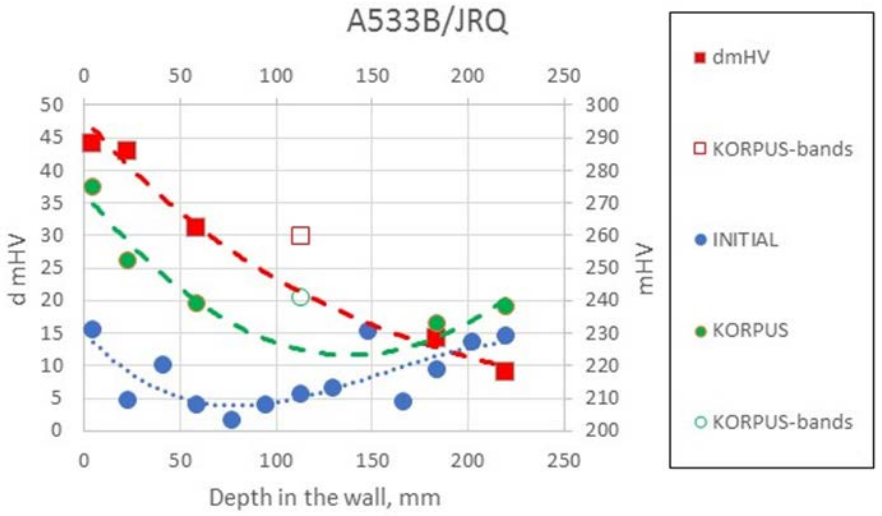

- 15Kh2NMFAA
  - Irradiation-induced increase of HV0.1

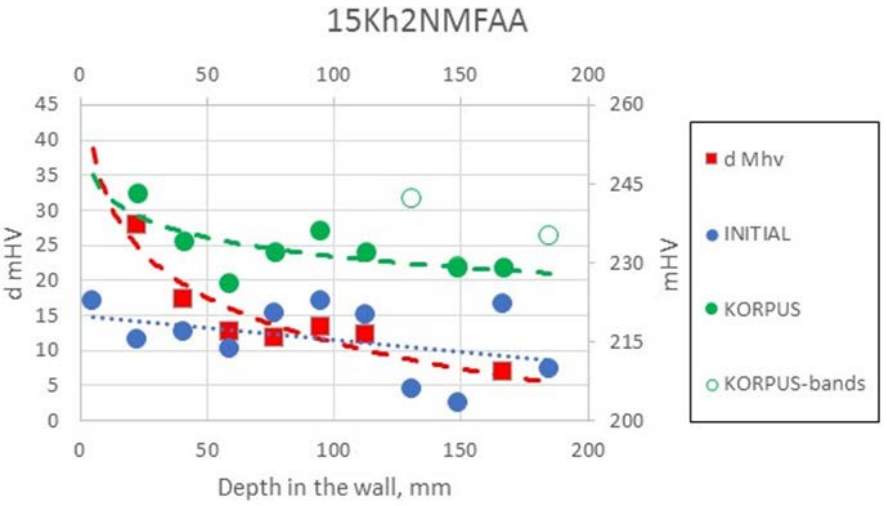

EDF-4, NRI-1, NRI-2: conclusions

- Segregation bands clearly identified
- Irradiation-induced nanofeatures and hardness increase observed
- Segregation-free areas, microsegregations and macrosegregations
  - exhibit different microstructures and hardness
  - do not exhibit differences in the irradition response
- Differences in the fracture behaviour (irr. versus unirr.) have not been addressed but are expected

ANP/VTT: basic information (1)

- Four irradiated materials were investigated:
  - PWR 22NiMoCr3-7 base materials ANP-3 and ANP-4 (Klöckner)
  - VVER-440 10KhMFT weld materials VTT-1 and VTT-MW1

	C	Si	Mn	P	S	Cr	Mo	Ni	Al	Co	Cu
ANP-3	0.23	0.20	0.70	0.015	n.s.	0.44	0.79	0.98	n.s.	n.s.	0.12
ANP-4	0.182	0.234	0.926	0.005	0.005	0.408	0.478	0.886	0.020	0.012	0.062
VTT-1	0.04	0.6	1.06	0.02	0.026	1.57	0.46	0.13	n.s.	n.s.	0.19
VTT-MW1	0.05	0.4	1.2	0.038	0.011	1.4	0.49	0.14	n.s.	n.s.	0.17

- Fractographic examination focused on
  - finding the primary cleavage initiation site
  - identifying any microstructural features or heterogeneities that may have promoted fracture in the irradiated condition.

ANP/VTT: basic information (2)

- ANP samples investigated: ⊕

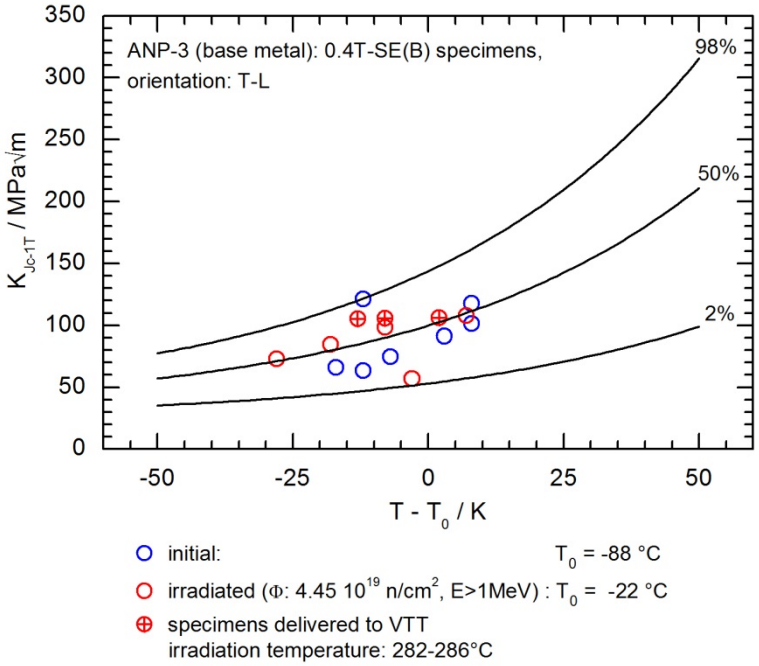

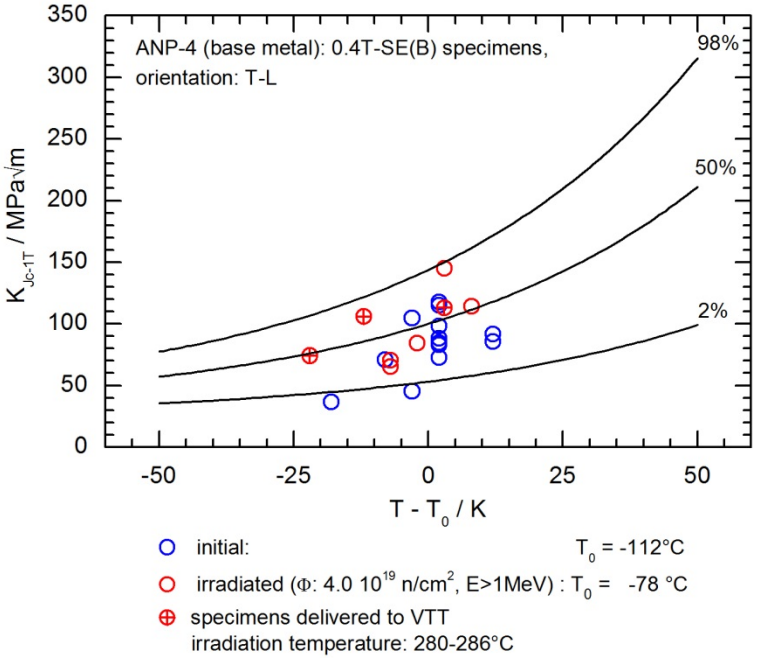

- Optical, fractography, SEM-EDS performed at VTT

ANP/VTT: initiation sites (1)

- ANP-3
  - left: overview (cleavage initiation site marked)
  - middle: cleavage initiating particle (marked)
  - right: spots for SEM-EDS analysis

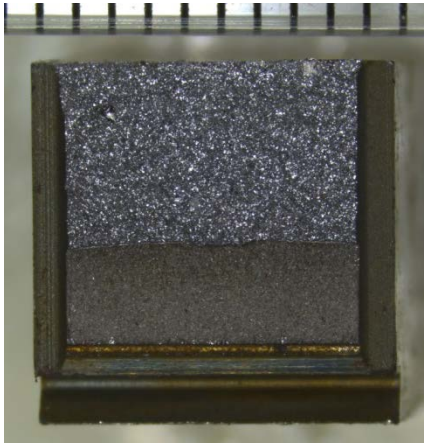

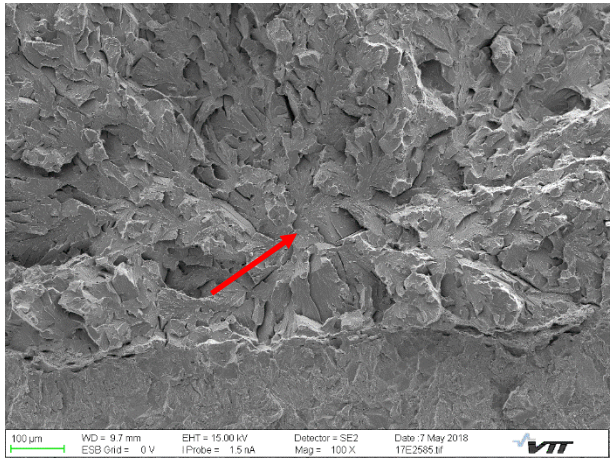

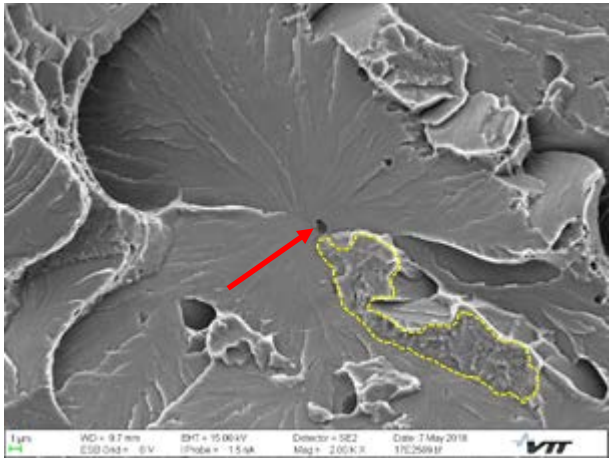

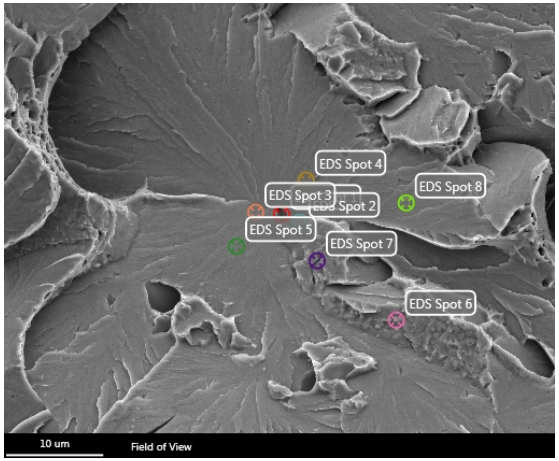

ANP/VTT: initiation sites (2)

Material	Specimen	Cleavage initiation site	Type of initiating particle
ANP-3	BA28	Primary Initiation site Not visible, as it locates under a ledge	No visible particle
ANP-3	BA32	Primary initiation site particle	Cr-, Mn-, Mo- (+ S), Co- and O-rich particle Cr, Mn, Co = half A Mo (+ S), O = half B
ANP-3	BA35	Primary initiation site particle	Probably a Mn-, Cr-, Mo- (+ S), Al-, O-rich particle half A only no particle on half B
ANP-4	2BTL3	Primary initiation site	No clear particle
ANP-4	2BTL9	Primary initiation site particle	Probably a Mn-, Mo- (+ S), S-, Cr-, C- and O-rich particle Mo (+ S), Cr, Mn, O = half A Mo, S, Cr, Mn, O = half B
ANP-4	2BTL14	Primary initiation site	No particle visible
VTT-1	L22_17I209	Initiation site	No particle visible
VTT-1	L22_18I204	Initiation site Particle	Al-, Si-, S-, Ti-, Mn- and O-rich particle
VTT-1	L24_17I204	Initiation site Particle	Al-, Si-, Ti-, Mn- and O-rich particle
VTT-MW1	132M	Initiation site Particle	Al-, Si-, Ti-, V-, Mn- and O-rich particle
VTT-MW1	172	Initiation site Particle	Al-, Si-, Ti-, Mn- and O-rich particle
VTT-MW1	311	Initiation site Particle	Si- and O-rich particle

ANP/VTT: conclusions

- Initiation sites identified and distance from the sample side face statistically evaluated
- ANP-3 and ANP-4
  - in three out of 6 cases visible particles enriched with Cr, Mn, Mo (S), Al, O
  - initiating particles might be MnS or Cr-, Mn-, Al-oxides or combinations of both
- VTT-1 and VTT-MW1
  - initiating particles typically Al-, Si-, Ti-, Mn-, O-rich
- Initiation at carbides was not reported

Task 3.3: lessons learned

- Six partners – eight materials – four approaches – many pieces of new insight
- Initial inhomogeneity may be
  - alleviated by irradiation (scatter of MC decreased)
  - retained after irradiation (segregated and segregation-free areas exhibit similar irradiation response, IGF)
  - intensified by irradiation (no example found → good message)
- Remaining gaps (personal view)
  - systematically correlate outliers in MC curves with local microstructure (segregated or segregation free-areas)
  - systematically compare initial distribution of coarse particles with type of particles initiating cleavage